REPORT DOCUMENTATION PAGE

Form Approved
OMB No. 0704-01-0188

PLEASE DO NOT RETURN YOUR FORM TO THE ABOVE ADDRESS.

1. REPORT DATE *(DD-MM-YYYY)*	2. REPORT TYPE	3. DATES COVERED *(From - To)*
26-04-2006	REPRINT	

4. TITLE AND SUBTITLE

Reexamination of ionospheric chemistry: high temperature kinetics, internal energy dependences, unusual isomers, and corrections

5a. CONTRACT NUMBER

5b. GRANT NUMBER

5c. PROGRAM ELEMENT NUMBER
61102F

6. AUTHORS

A.A. Viggiano

5d. PROJECT NUMBER
2303

5e. TASK NUMBER
BM

5f. WORK UNIT NUMBER
A1

7. PERFORMING ORGANIZATION NAME(S) AND ADDRESS(ES)

Air Force Research Laboratory /VSBXT
29 Randolph Road
Hanscom AFB, MA 01731-3010

8. PERFORMING ORGANIZATION REPORT NUMBER
AFRL-VS-HA-TR-2006-1059

9. SPONSORING/MONITORING AGENCY NAME(S) AND ADDRESS(ES)

10. SPONSOR/MONITOR'S ACRONYM(S)
AFRL/VSBXT

11. SPONSOR/MONITOR'S REPORT

12. DISTRIBUTION/AVAILABILITY STATEMENT
Approved for public release; distribution unlimited.

13. SUPPLEMENTARY NOTES
Reprinted from Physical Chemistry Chemical Physics, 2006, Vol 8. © 2006 the Owner Societies

14. ABSTRACT A number of aspects of ionospheric chemistry are revisited.
The review discusses in detail only work performed at AFRL, but other work is mentioned. A large portion of the paper discusses measurements of the kinetics of upper ionospheric reactions at very high temperatures, *i.e.* the upper temperature range has been extended to at least 1400 K and in some cases to 1800 K. These temperatures are high enough to excite vibrations in O_2, N_2, and NO and comparing them to drift tube data allows information on the rotational temperature and vibrational level dependences to be derived. Rotational and translational energy are equivalent in controlling the kinetics in most reactions. Vibrational energy in O_2 and N_2 is often found to promote reactivity which is shown to cause ionospheric density depletions. NO vibrations do not significantly affect the reactivity. In a number of cases, detailed calculations accompanied the experimental studies and elucidated details of the mechanisms. Kinetics fo two peroxide isomers important in the lower ionosphereic have been measured for the first time, *i.e.* NOO^+ and $ONOO^-$. Finally, two examples are shown where errors in previous data are corrected.

15. SUBJECT TERMS

Ionospheric chemistry	High temperature
Vibrational effects	Unusual isomers

16. SECURITY CLASSIFICATION OF:			17. LIMITATION OF ABSTRACT	18. NUMBER OF PAGES	19a. NAME OF RESPONSIBLE PERSON
a. REPORT	b. ABSTRACT	c. THIS PAGE			A. A. Viggiano
UNCL	UNCL	UNCL	UNL		19B. TELEPHONE NUMBER *(Include area code)*

Reexamination of ionospheric chemistry: high temperature kinetics, internal energy dependences, unusual isomers, and corrections

A. A. Viggiano

Received 9th March 2006, Accepted 3rd April 2006
First published as an Advance Article on the web 26th April 2006
DOI: 10.1039/b603585j

A number of aspects of ionospheric chemistry are revisited. The review discusses in detail only work performed at AFRL, but other work is mentioned. A large portion of the paper discusses measurements of the kinetics of upper ionospheric reactions at very high temperatures, *i.e.* the upper temperature range has been extended to at least 1400 K and in some cases to 1800 K. These temperatures are high enough to excite vibrations in O_2, N_2, and NO and comparing them to drift tube data allows information on the rotational temperature and vibrational level dependences to be derived. Rotational and translational energy are equivalent in controlling the kinetics in most reactions. Vibrational energy in O_2 and N_2 is often found to promote reactivity which is shown to cause ionospheric density depletions. NO vibrations do not significantly affect the reactivity. In a number of cases, detailed calculations accompanied the experimental studies and elucidated details of the mechanisms. Kinetics of two peroxide isomers important in the lower ionospheric have been measured for the first time, *i.e.* NOO^+ and $ONOO^-$. Finally, two examples are shown where errors in previous data are corrected.

Introduction

In the 1960's and 1970's the ion chemistry of the ionosphere was studied extensively and many of the important properties elucidated.[1–4] However, the measurements did not extend to all relevant conditions and to all species. Temperature dependences were often lacking or extended over only part of the pertinent range.[5–8] Product state information was only occasionally known.[9–11] The maximum temperature studied was below that for which vibrational excitation of N_2, O_2, and NO occurred.[12] As shown later, this is important. Additionally, the ionosphere is often not in temperature equilibrium meaning that translational and internal temperatures are not the same. Correct modeling of ionospheric chemistry therefore requires knowledge of how each individual type of energy effects reactivity.[10,13] Modern experimental and theoretical techniques allow for more complete coverage of the chemistry and many previously unknown details of the mechanisms can now be revealed.

This review will discuss advances made in the plasma chemistry laboratory at the Air Force Research Laboratory in furthering the understanding of the chemistry of the ionosphere. While mention will be made about contributions made elsewhere, this review will not cover those in detail since it is already quite long. Also in an attempt to limit the length of the review, only highlights of what the measurements revealed are given. The original papers can be used to learn the details. One unique aspect of the AFRL instrumentation is the ability to study kinetics over a large range, 90–1800 K. The upper limit is double that of previous studies and covers most of the ionospheric range and therefore the review will emphasise information learned by studying temperature dependences over very wide ranges. The low range can be extended downward in other laboratories by the CRESU and trap techniques.[14–19] While going to lower temperatures helps in interpreting mechanisms, it is more important for interstellar chemistry than for ionospheric chemistry.

Not only has the ionospheric chemistry been remeasured at AFRL over wider ranges of temperatures, but information on how rotational and vibrational energy affects reactivity can also be derived by a comparison to drift tube data taken as a function of kinetic energy.[20,21] Advances have also been made in product state identification and examples will be discussed. However, other laboratories are better at such studies.[19,22–26] Reactivity of two unusual peroxide isomers will be presented, namely NOO^+ and $ONOO^-$. While these ions were discovered elsewhere,[27,28] the previous experiments were not able to study the chemistry of these species or in the case of NOO^+ to unambiguously determine its structure.[29–31] Finally, two examples of corrections to previous data are presented.

Fig. 1 shows a schematic of the ionosphere total charge density and temperatures.[32,33] Conditions vary considerably and should be used only as guidelines. The graph indicates three regions that have density plateaus or maximums, the so-called D, E, and F regions. Some of these have sub-maxima. Typical terminal ions are shown which become more complex with decreasing altitude. Three different temperatures are shown, *i.e.* ion, electron, and neutral. These refer to average conditions for a typical mid-latitude day. At lower altitudes the ion and neutral temperatures are similar. Conditions can vary considerably with magnetic latitude and whether a solar storm is occurring. These are meant only as a rough guide.

The ionospheric chemistry involves mainly species containing only N and O atoms, especially in the mid (E-region) and upper (F-region) ionosphere. Fig. 2 shows the chemistry

Air Force Research Laboratory, Space Vehicles Directorate, 29 Randolph Rd., Hanscom Air Force Base MA 01731-3010, USA

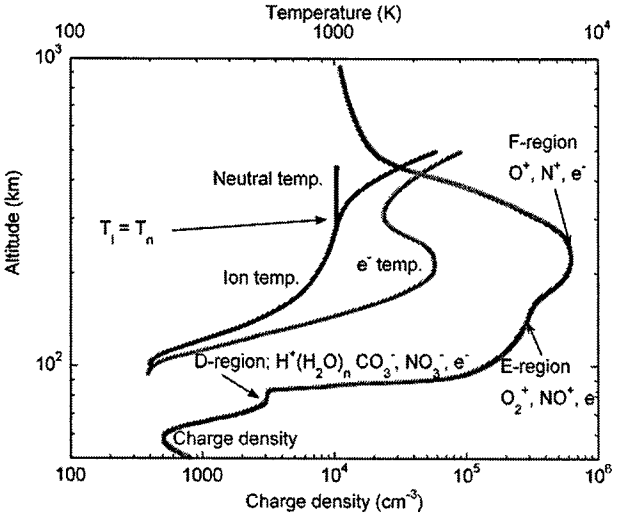

Fig. 1 Schematic of ionospheric temperatures and charge density *vs.* altitude. The temperatures are from Jasperse[32] and the density profile from Viggiano and Arnold.[33]

involving only species with one or two N and/or O atoms, which covers the main reactions in those regions. This three-atom chemistry is even more complex than shown because the figure does not include the various excited states that are also important. Under non-ionospheric storm conditions, the chemistry starts by photoionization and electron impact ionization of the main constituents, N_2, O_2, N, and O to produce their parent ions. In ionospheric storms involving high energy electrons, high energy electron impact produces not only the parent ions but also O^+ and N^+ from O_2 and N_2. The high energy electrons are shown with an asterisk. The only other ion species shown is NO^+, which in the upper ionosphere can be considered the most stable ion, *i.e.* is unreactive. (In the lower ionosphere, metals, proton hydrates, and negative ions are also important.[34–37]) All ion molecule reactions shown in Fig. 2, except those involving O atoms, have been studied at AFRL to temperatures of at least 1400 K and sometimes 1800 K. At these temperatures, vibrational excitation of the diatomic species occurs and the comparison to drift tube data allows the state specific vibrational rate constant to be deduced for the tri-atom systems.

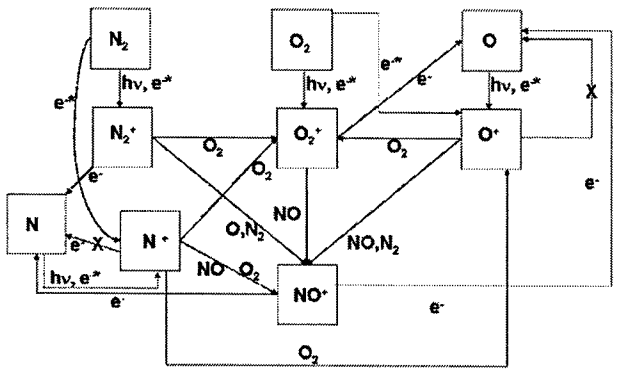

Fig. 2 Chemical pathways of the upper ionosphere.

Particularly important are those reactions that convert monatomic to diatomic ions since the former recombine only slowly with electrons and the latter recombine rapidly. While the recombination rate constants have been known for a long time, technique advances in studying recombination now allow for product state information and dependences on the vibrational or electronic state of the ion to be obtained. These important studies have been performed elsewhere and are not further discussed.[38–43]

As altitude decreases and pressure increases, more complicated positive ions, as well as negative ions, are formed. This switchover occurs mainly in the mesosphere/D-region. To help understand this chemistry, we have studied in detail the chemistry of NOO^+ and $ONOO^-$ for the first time. At higher pressures in both the atmosphere and atmospheric discharges, N_3^+ forms and the reactivity of that ion with O_2 and NO has been studied in detail.

In the stratosphere and troposphere, the chemistry quickly produces clusters with H_3O^+ and NO_3^- cores.[33] At that stage the chemistry mainly involves proton transfer to bases for positive ions and from acids for negative ions. The reactivity is mainly determined by thermodynamics and is not discussed here.[44]

Experimental

The experiments were performed in two fast flow tubes at the Air Force Research Laboratory. The first is the selected ion flow drift tube (SIFDT) which is shown in Fig. 3.[20,45] In this apparatus, ions are created in a moderate pressure ion source (~0.1–1 Torr) through electron impact or alternatively for cluster ions by ionizing a supersonic expansion.[44] The source is in a differentially pumped chamber. The mix of ions created is extracted and injected into a quadrupole mass filter where the ion of interest is selected and injected into the flow tube. A Venturi inlet is used to aid in introducing ions from the low pressure quadrupole chamber ($\sim 10^{-4}$ Torr) to the higher pressure flow tube (~0.4 Torr). The use of the Venturi aids in reducing the ion velocity needed to circumvent the pressure differential which reduces breakup and vibrational excitation of the ions.

Once in the flow tube, the ions quickly thermalize with the buffer gas. The buffer gas, usually helium, carries the ions downstream. The bulk of the gas is pumped by a Roots type blower and small fractions of the gas and ions are sampled

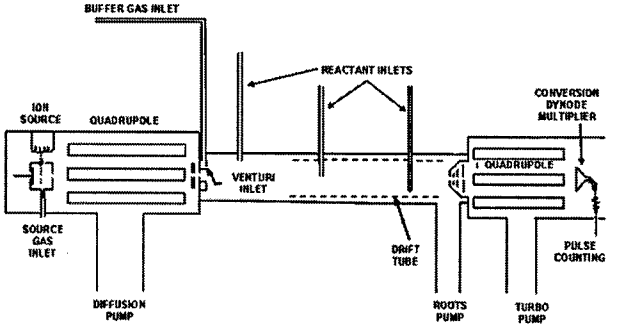

Fig. 3 Schematic of the selected ion flow drift tube.

through a small hole in a truncated nose cone. The ions then enter a second quadrupole mass spectrometer and are detected by a particle multiplier.

One notable exception to the ions being thermalized is vibrational relaxation of diatomic and some cases triatomic ions. Helium is a very inefficient quencher for species with only high vibrational frequencies.[46] In those cases, a non-reactive quench gas is added to the buffer to thermalize the vibrations. For example, O_2 neutrals rapidly quench O_2^+ through a charge exchange process. Approximately one half of the flow tube is used for thermalization. Occasionally, the ion of interest cannot be made in the ion source. The upstream end of the flow tube is then used to change the identity of the ion by injection of a reactive gas upstream of the reaction region. An example is $ONOO^-$, which is made through the reaction of CO_4^- with NO.[47]

Once the ions are thermalized, a neutral reagent is added between 35 and 55 cm from the end of the flow tube and allowed to react with the primary ion. Rate constants are measured by monitoring the exponential decay of the primary ion as a function of the flow rate of the reactant neutral. Rate constants are derived from the decay with the knowledge of the neutral concentration and the reaction time. Branching fractions are obtained by extrapolating the fractional abundance of each product ion to zero neutral concentration. The extrapolation takes into account any potential secondary chemistry. Obtaining nascent branching fractions is still problematic when the secondary chemistry is about 10 times faster than the primary chemistry. The neutral concentration is straightforward to determine by measuring flow rates and the flow tube pressure. The derivation of the reaction time is discussed below.

The entire flow tube can be heated or cooled to allow for measurements as a function of temperature. In the past, the temperature range of the SIFDT was 90–550 K. It is important to pre-cool the buffer gas in order to obtain accurate measurements at low temperature.[48] However, preheating is not needed since heat transfer is more efficient at high temperature.[49] At the time of this writing, the flow tube has been replaced with one that can be heated to 900 K but that feature has not been tested yet. The higher temperature is obtainable by ridding the system of low temperature seals and Teflon wires.

A drift tube is sometimes inserted into the flow tube to allow for measurements as a function of kinetic energy. The drift tube consists of 60 rings that are 9 mm wide with a 1 mm gap. Wires from each ring are connected to an external resistor chain. Applying a voltage across this resistor chain allows a uniform electric field to be applied to the drift tube, thereby accelerating the ions. For monatomic ions, the translational degrees of freedom quickly reach steady state such that a quasi-Boltzmann distribution of ion energies is established.[50–54] Drift tube measurements can be performed over the entire previous temperature range of the instrument.

The reaction time is determined by measuring the ion velocity and the reaction distance. A complication in knowing the reaction distance is that it is not feasible to introduce the neutral reagent in such a way that the concentration is immediately uniform across the flow tube. Instead diffusion evens out the concentration over a non-negligible distance, referred to as the end correction. Measurements at two reactant distances allow the end correction to be derived since the true rate cannot vary with reaction distance. The rates measured at the two distances are forced to be equal by adjusting the reaction distance (and therefore time) by an equal amount since the two inlets are essentially identical.

Two types of inlets are used. A finger inlet, which is a 1/8″ tube truncated at the center of the flow tube pointing upstream, is used much of the time if the kinetics parameters are measured without the drift tube. End corrections for these inlets are small, usually negligible without an applied field.[45,55,56] However, when making measurements as a function of kinetic energy, the end correction varied dramatically with the applied field and were non-physical at higher fields.[55,56] Therefore, ring inlets are used when the drift tube is inserted. The ring inlets consist of a ring of 1/8″ tubing positioned at half the radius of the flow tube with a number of small holes facing upstream. The end corrections are generally 3–12 cm and depend only weakly on the electric field. The best explanation for the almost zero end correction for the finger inlets is that it stems from the cancellation of two effects: (1) it takes a large distance for the neutral reagent to mix thoroughly and (2) the ion concentration is highest on the centerline where the neutral concentration is also highest near the inlet. This causes a "hole" in the ion concentration at the center of the flow tube. Without the electric field there is sufficient time for the ions to diffuse back to the center and with the electric field there is not.

The other parameter necessary for accurate measurements of the reaction time is the ion velocity. This is not simply the buffer velocity[57] since (1) the buffer velocity has a parabolic profile where the centerline velocity is twice the average and is near zero at the wall. (2) Ions are lost to the wall on essentially every collision. Thus, on average the ion velocity is greater than the average neutral velocity. When the drift tube is inserted, the ion velocity is measured for every condition by pulsing two of the rings to determine the arrival times of the ion disturbance at the detector. Subtracting the two times and knowing the distance between the two rings yields the ion velocity. Pulsing two rings and subtracting corrects for any end effects. In essence, the ion mobility[54,58,59] is measured and several such measurements have been reported.[60,61] Without the drift tube, this same technique was used, but two finger inlets were pulsed. The zero field measurements were made over a wide range of conditions and parameterized so that they do not need to be measured routinely.

By measuring all these parameters, it is estimated that rate constants can be measured with a 25% accuracy and 15% relative accuracy, which is the rate at one condition compared to another for the same reaction.[45]

The other instrument used in these studies is a high temperature flowing afterglow (HTFA) with a temperature range of 300 to 1800 K.[21,62] In principle the instrument operates in a similar manner to the SIFDT, so here the differences between the two are emphasized. The high temperature range is reached by inserting the flow tube into a commercial furnace with three zones. In this instrument, the buffer gas starts cold

and reaches temperature equilibration before the reactant neutral is added.[49]

The other main difference between the instruments is that in the HTFA the ion source in located in the flow tube and mass selection is not possible. This is necessary since hot metal is highly reactive with most neutral gases necessitating the flow tube to be made of industrial quartz for temperatures up to 1400 K or alumina for temperatures up to 1800 K. The quartz tube is most often used since the alumina tube is also reactive, *e.g.* with NO at temperatures greater than 1000 K.[63] The non-conductive nature of the flow tubes means that it is not practical to have an ion swarm of one sign since the flow tube would charge and the resulting electric field would disturb the ions. Thus, a bipolar swarm is needed and a nonselective source is required. In the present version of the instrument, the source is housed in a short sidearm upstream of the furnace and consists only of a biased filament that ionizes the helium buffer gas. The He^+ ions as well as helium metastables then react with the source gas to produce the ions of interest. This region is separated from the main flow tube by a diaphragm in order to have as much as possible of the production of the primary ion occur in the source. A source pressure up to tens of Torr is achieved if a small hole is used. This is desirable for reducing the amount of gas needed but if the primary ion is reactive, larger holes are used to prevent unwanted chemistry. Having the source in a sidearm also prevents UV light from reaching the detector and creating ions in the reaction region.

All electrical and gas feedthroughs are in the upstream cold region. This requires that the gas lines sit at the bottom of the flow tube and the inlets have a right angle bend so that they operate like the finger inlets described for the SIFDT. In the upstream "cold" region normal seals can be used. The downstream end of the furnace and flow tube simply abuts a cooled detector housing. Therefore, appreciable leaks are present. To ensure that the leaks are out of the flow tube and not in, the entire system is in a separate vacuum chamber pumped by a second Roots type blower. In this manner, the leaks are controlled and not important since most of the gas still flows into the primary Roots type blower.

Velocity and end corrections were measured once since these measurements are quite tedious in this system and require removing some of the inlets. Rate constants were found to be the same within error in the overlapping temperature range of the SIFDT and HTFA. The good agreement is obtained in part because important parameters including the ion velocity have been measured. The ability to go to 1800 K doubled the previous high temperature ion-molecule measurements made at NOAA and the University of Pittsburgh.[7,8] Recently, measurements at high temperatures have been made for Ca^+ reactions in a high pressure photo-reactor in the Fontijn laboratory. The first publication is expected shortly.[64]

The ability to study kinetics as a function of temperature and kinetic energy allows information on internal energy dependences to be derived.[20,21] Of course, in pure temperature measurements all degrees of freedom are in thermal equilibrium and Maxwell–Boltzmann distributions apply. In a drift tube experiment, several distributions are important. Rotational and vibrational distributions of the reactant neutral are simply determined by the buffer gas temperature. In a drift tube the average kinetic energy in the center of mass frame is given by the Wannier expression,[54,59,65]

$$\langle KE_{CM} \rangle = \frac{(m_i + m_b)}{2(m_i + m_n)} v_d^2 + \frac{3}{2} kT \qquad (1)$$

where m_i, m_b, and m_n are the masses of the reactant ion, buffer gas, and reactant neutral, respectively, v_d is the reactant ion drift velocity, and T is the temperature. In the SIFDT, v_d is the difference in the measured ion velocity with the field on and off, *i.e.* the added velocity due to the electric field.[66]

Not only is the average energy important, but also is the energy distribution. Fortunately, the kinetic energy distribution in a helium buffer is quasi-Maxwellian and the kinetic temperature (T_{eff}) is therefore derived simply from $\langle KE_{cm} \rangle$ = 3/2 kT_{eff}. Quasi-Maxwellian implies that rate constants measured with the actual distribution differ by less than 10% from what would be measured if the distribution was truly Maxwell–Boltzmann.[50–54,67] This is true even for reactions with very steep kinetic energy dependences.

If the ion is monatomic, the distributions described above are the only ones that matter. Therefore, when data with the same average translation temperature (or equivalently average kinetic energy) but with differing contributions from the drift field and temperature are compared, the difference is due to the internal modes of the neutral. If the vibrational frequencies of a neutral molecule are large and therefore not excited, then pure rotational temperature dependences can be derived. This is the case for most diatomic molecules at lower temperatures (<900 K). This technique has produced more information on how rotational energy affects ion molecule kinetics than any other.[20,21,68] Of course, it is not state selected but reflects rotational temperature dependences. By extrapolating the rotational dependences to temperatures where vibrational excitation becomes important, it is possible to derive state selected rate constants for v = 0 (pure drift tube data) and v = 1 and sometimes v = 2. Examples are given in the Discussion section.

If polyatomic ions are involved, one also needs to know the internal energy distributions of the ions. These can be approximated by using the average kinetic energy of the ions with respect to the buffer gas, $\langle KE_{cm} \rangle_{buf}$, instead of the reactant neutral. $\langle KE_{cm} \rangle_{buf}$ is derived by substituting m_b for m_n in eqn (1).[54,69] The internal modes of the buffer are then given by distributions involving a T_{eff}(int) derived from $\langle KE_{cm} \rangle_{buf}$ = 3/2 kT_{eff}(int). This holds for polyatomic ions, but may be in error for vibrational excitation in diatomic molecules for which the excitation rate is slower.[70] At low fields, little excitation of diatomic vibrations occurs in any case. When one of the reactants is polyatomic, information on individual types of energy is usually not possible and only information on the total energy dependence can be derived. There are exceptions but these often involve some simplification and are only possible for species with uniformly high vibrational frequencies, *e.g.* CH_4. For information on how the vibrational energy of ions changes reactivity, experiments involving multiphoton ionization in beam machines are often more informative.[71–85] However, for information on how internal energy of the neutral reagents affects the reactivity or for information on rotational energy, the flow tube technique described above

appears to be the most easily applied technique, although a few studies used other means.[86,87]

In interpreting the comparison of temperature and drift tube data, three types of plots have proven useful. The starting place is of course a plot of rate constant or branching ratios *vs.* $\langle KE_{cm} \rangle$ or equivalently translational temperature. In this type of plot, any difference between pure temperature data and drift tube data in the vertical direction indicates an internal energy dependence. The next step is to make a plot of the kinetic parameter *vs.* the sum of the average kinetic and rotational energy. In systems where vibrational excitation is unimportant, this tests how rotational energy might differ from translational energy. In almost every case, the two forms of energy behave similarly, especially if the molecule does not have a large rotational constant.[45,88,89] This equivalency allows extrapolation to somewhat higher temperatures, where vibrational excitation becomes important. With that assumption, differences on plots of this type are due to vibrational excitation and allow state specific rate constants to be derived. The drift tube data taken at low temperatures, where no vibrational excitation occurs, represent the $v = 0$ rate constant. The temperature data can be represented by a series expansion of the population of each state, fr_i, times the rate constant for that state, k_i, or $k = \Sigma_i fr_i k_i$. The populations are calculated from statistical mechanics. Combining the high temperature data with the $v = 0$ rate then yields information on how excited states behave. In practice, this technique is most sensitive when large positive changes in rate constants occur with increasing vibrational level.

Finally, a graph *vs.* average total energy determines if the reaction behaves statistically.[90–92] In the statistical case, dependences as function of kinetic energy and temperature coincide. This is most useful for larger systems where the details of rotational and vibrational effects are not possible to deconvolute. Examples of all three types of graphs will be shown. In practice, $\langle KE_{cm} \rangle$ dependences are not always measured at AFRL. Instead, previously measured data are used. Early measurements found that when reproducing such data, especially those from the prolific NOAA laboratory, essentially perfect agreement was usually found (<10% or so).

Results and discussion

High temperature chemistry

A particularly tutorial system for understanding the derivation of internal energy effects, as well as an ionospherically important one, is the charge transfer reaction of O^+ with O_2. This is one of two reactions studied to 1800 K.[93] In Fig. 4, the rate constants obtained in the HTFA are compared to data taken at NOAA at temperatures up to 900 K,[7] and those obtained as a function of average kinetic energy.[67] The data from the two temperature studies agree very well except perhaps at 900 K. The rate constants decrease with temperature from 100 to 700 K. From about 700 to 1200 K, a minimum in the rate constant is observed at a value of about 9×10^{-12} cm^3 s^{-1}. Above this temperature, the rate constants rise rapidly with temperature. The worth of the HTFA is clear

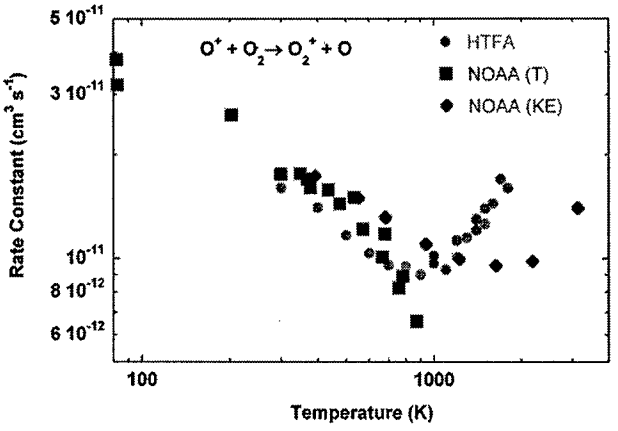

Fig. 4 Rate constants for the reaction of O^+ with O_2 as a function of temperature. The closed circles are HTFA data,[153] the closed squares are from Lindinger *et al.*[7] and the solid diamonds from McFarland *et al.*[58] Reprinted from *Advances in Gas Phase Ion Chemistry*, **4**, A. A. Viggiano and S. Williams, Ion–molecule kinetics at high temperatures (300–1800 K): Derivation of internal energy dependences, p. 85, copyright 2001, with permission from Elsevier.

from this comparison since the lower temperature data miss the upturn.

The drift tube data (converted to effective translational temperature) are a little higher than the HTFA data at low temperature, *i.e.* the translational temperature dependence for the drift tube data is less negative than the true temperature dependence. In contrast, the drift tube data are lower at high translational temperature and the upturn occurs at a higher effective temperature. This may seem contradictory. Replotting the data (in Fig. 5) as a function of average kinetic plus rotational energy clarifies the situation.[21] In Fig. 5 the drift tube data are scaled by 0.88 so that the 300 K points overlap. This 12% correction is well within the error of either measurement and agreement is usually this good or better. In Fig. 5 the HTFA and drift tube data below 0.2 eV agree almost exactly. This indicates that rotational and translational energy affect the rate constant to the same degree, at least in an average sense. This pattern has been found in dozens of reactions. The only definitive exceptions are for reactions where the rotational constant is quite large.[20,21,45,89,94] Large rotational constants and low temperature allows one to observe changes as molecules change from non-rotating ($J = 0$) to rotating, where large effects may be expected and indeed are sometimes observed.

In Fig. 5 the higher energy points diverge; the pure temperature rate constants are greater than those measured in the drift tube. This is a consequence of vibrational excitation of O_2 at high temperatures. The rate constants for O_2 ($v = 0$) are just those measured in the drift tube. Since the pure temperature rate constants can be written as $\Sigma_i fr_i k_i$ and the fr_i can be calculated easily, it is possible to calculate the rate constants for vibrationally excited O_2 if one assumes that all vibrationally excited states react equally and that the equivalence of translational and rotational energy hold at slightly higher energies. In the $O^+ + O_2$ reaction, the divergence of the drift tube and HTFA data occurs at temperatures above the point where $v = 1$ is excited and approximately where $v = 2$

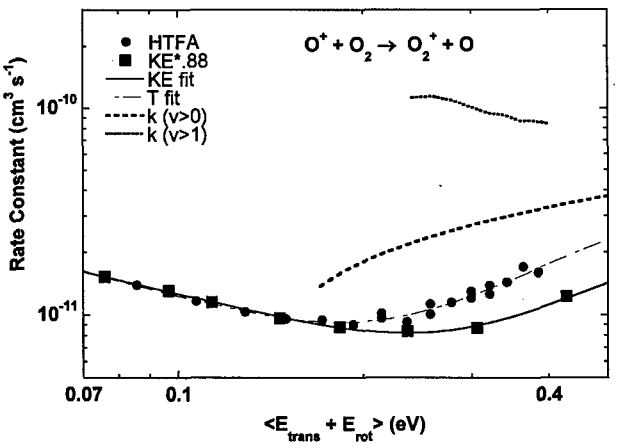

Fig. 5 The data from Fig. 3, replotted as a function of average translation plus rotational energy. Reprinted from *Advances in Gas Phase Ion Chemistry*, **4**, A. A. Viggiano and S. Williams, Ion–molecule kinetics at high temperatures (300–1800 K): Derivation of internal energy dependences, p. 85, copyright 2001, with permission from Elsevier.

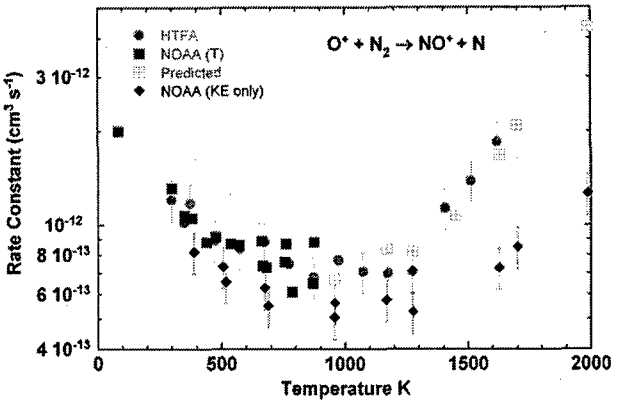

Fig. 6 Rate constants for the reaction of O^+ with N_2 as a function of temperature. The HTFA,[153] NOAA (T),[7] and NOAA (KE)[58] data are shown as circles squares and diamonds, respectively. Reprinted from *Advances in Gas Phase Ion Chemistry*, **4**, A. A. Viggiano and S. Williams, Ion–molecule kinetics at high temperatures (300–1800 K): Derivation of internal energy dependences, p. 85, copyright 2001, with permission from Elsevier.

becomes populated. Therefore, excited state data are derived in two ways; (a) $v = 1$ molecules are assumed to act the same as those in $v = 0$ ($k_0 = k_1 \neq k_2 = k_3 \ldots$) and (b) where $v = 1$ molecules are assumed to behave like $v = 2$ and higher states ($k_0 \neq k_1 = k_2 = k_3 \ldots$). The derivations for both scenarios are shown in Fig. 5. In case b the higher order states increase reactivity by a factor of about 10 and in case a the enhancement is less than a factor of three. While the case b is likely since the enhancement occurs at the point where $v = 2$ becomes populated, the data are not sufficiently detailed to be definitive. The fits in the figure use a power law (decline) + exponential (increase) dependence.

Other charge transfer reactions involving O_2 behave similarly, *i.e.* reactions with N_2^+ and Ar^+. The similarity is in the magnitude of the rate constants, the shape of the curves and the magnitude of the rate enhancement for vibrationally excited states. Franck Condon arguments are the most obvious explanation although the exothermicities of the reactions vary substantially.[95,96]

The most important reaction in the ionosphere is the reaction of O^+ with N_2,

$$O^+ + N_2 \rightarrow NO^+ + N. \qquad (2)$$

The importance stems from several details including the abundance of O^+ and N_2 in the ionosphere and the fact that a monatomic ion is converted into a diatomic ion. As explained earlier, diatomic ions recombine much more rapidly than monatomic ions with electrons and therefore conversion to diatomic ions deplete the total electron concentration. Because of its importance, numerous studies of the kinetics of the reaction have been made including kinetic energy dependences,[58,67,97] two temperature studies up to 900 K,[7,8] and an outstanding study of the vibrational temperature dependence.[87] Since ionospheric temperatures can reach 2000 K, it is important to have measurements at as high a temperature as feasible. In part, the HTFA was built to study this reaction.

Rate constants for reaction 2 studied in the HTFA up to 1600 K are compared to several other measurements in Fig. 6. There again is good agreement with a previous study to 900 K. The HTFA data start to increase at 1400 K and again show that 900 K was not high enough for understanding the reactivity for all ionospheric conditions. The drift tube data show a shallower upturn at a higher effective temperature. Due to the very small rate constants, it is difficult to determine whether rotational and translational energy are equivalent in this reaction. In order to obtain an appreciable extent of reaction, large amounts of N_2 had to be added. This perturbs the helium flow slightly and the errors are probably about 10% larger than normal. The upturn at high temperatures is significantly outside the error limits and can be checked by comparing to measurements made as a function or vibrational temperature. This is the only reaction for which data above 900 K can be compared to measurements taken elsewhere. The open points with pluses inside are a convolution of the drift tube data and the vibrationally excited data. Excellent agreement is found with the HTFA high temperature results indicating that vibrational excitation is responsible for the upturn. Since the rate constants depend only slightly on translational energy in this regime and the error bars are a little larger, rotational energy has been ignored in that analysis. The upturn is mainly caused by $v \geq 2$ excitation.[87]

The importance of the increase in the rate constants for O^+ reacting with vibrationally excited O_2 and N_2 has recently been used to explain ionospheric satellite data related to sub-auroral density troughs.[98] In a density trough, the electron density decreases rapidly and causes communication problems since electrons interact with radiowaves. Analysis of the satellite data showed that the depth of the troughs was related to the electron and not ion temperature, *i.e.* they were caused by hot electrons. The mechanism used to explain the depletions is as follows. First, the hot electrons cause vibrational excitation in neutral O_2 and N_2. As shown above, the vibrationally excited neutrals react much more rapidly with O^+

than the ground vibrational states. The excitation increases the rate of conversion of the dominant atomic ion, O^+, to O_2^+ and NO^+. The diatomic ions recombine orders of magnitude faster with electrons than O^+ which produces the electron density depletion. When the electron temperature is below 2000 K not much effect is seen and when the temperature reaches 5000 K depletions on the order of a factor of 6 occur within 10 min after the energetic electrons appear.

Fig. 2 shows a number of other ionospheric reactions that have also been studied in the HTFA. As mentioned previously, the reaction of N_2^+ with O_2 is in many respects similar to the O^+ reaction and has been measured up to 1800 K.[99] Rotational and vibrational energies are also found to be equivalent in this reaction, showing that rotational energy in both the neutral and ion have the same effect as translational energy.

The reaction of N^+ with O_2 is the most important reaction that converts the minor ion, N^+, to a diatomic species. It produces three product ions although the reaction is even more complicated when one considers the states of the products,

$$N^+(^3P) + O_2(X\ ^3\Sigma_g) \rightarrow O^+(^4S) + NO\ (X\ ^2\Pi) + 2.3\ eV \quad (3a)$$

$$\rightarrow O_2^+\ (X\ ^2\Pi_g) + N(^4S) + 2.5\ eV \quad (3b)$$

$$\rightarrow NO^+\ (X\ ^1\Sigma^+) + O(^3P) + 6.7\ eV \quad (3c)$$

$$\rightarrow NO^+\ (a\ ^3\Sigma^+) + O(^3P) + 0.3\ eV \quad (3d)$$

$$\rightarrow O_2^+\ (X\ ^2\Pi_g) + N(^2D) + 0.04\ eV. \quad (3e)$$

While this reaction has been extensively studied previously,[7,9–11,58,100–108] several aspects of it have been worth reexamining. At AFRL the high temperature behavior of the rate constant[99,109] was measured as well as the first study of the temperature dependence of the branching ratio.[109] In addition, a better limit was placed on the production of $NO^+(a\ ^3\Sigma^+)$ and very detailed calculations of the reaction mechanism were made which yielded predictions of the probable neutral product states.[110]

The first attempt in our laboratory to measure the high temperature rate constant for this reaction was in error[99] because not enough N_2 was added to completely deplete He^+ by the beginning of the reaction zone. The previous study up to 900 K was in agreement with the original data and therefore also in error.[7] This agreement gave a false sense of confidence in the original data. However, the original data did not show the equivalency of translational and rotational energy. After data for many other systems showed this equivalency, the kinetics for the N^+ reaction with O_2 was remeasured. The new measurements revealed that the original HTFA rate constants indeed were in error.[109] The results are shown in Fig. 7. Rate constants are about 50% of the collisional value and flat at low temperature and as a function of the kinetic energy.[58] This again shows that translational and rotational energy are equivalent. At higher temperatures, the rate constants are slightly higher than those with the same kinetic temperature. The difference is just about at the relative error limit and is consistent with an increase in the rate constant for vibrationally excited molecules to the collisional value. This could imply that the charge transfer channel increases for $v = 1$, since it is often charge transfer that shows

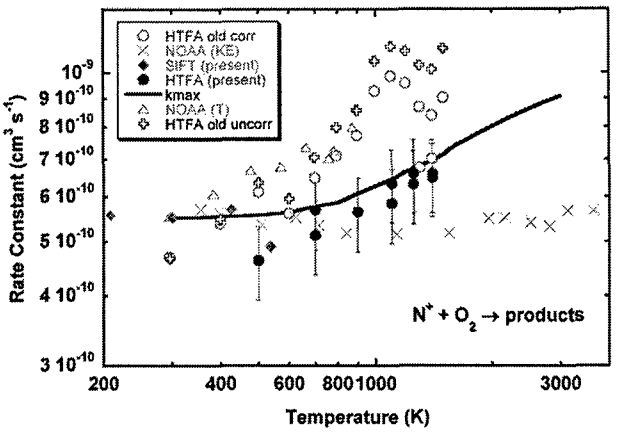

Fig. 7 Rate constants for the reaction of N^+ with O_2 as a function of temperature. The SIFT and HTFA points are from Viggiano *et al.*[109] The NOAA kinetic energy (KE) data are from McFarland *et al.*,[58] the temperature data NOAA(T) are from Lindinger *et al.*[7] The HTFA old corr and HTFA old uncorr refers to the published HTFA data.[99] The correction is a small one due to thermal transpiration. Reprinted from *International Journal of Mass Spectrometry*, **223–224**, A. A. Viggiano, W. B. Knighton, S. Williams, S. T. Arnold, A. J. Midey and I. Dotan, A reexamination of the temperature dependence of the reaction of N^+ with O_2, pp. 397–402, copyright 2003, with permission from Elsevier.

large vibrational effects especially in reactions involving O_2. Unfortunately it is not possible to produce N^+ pure enough so that branching ratio data could be taken for this reaction above 550 K (the previous SIFDT limit).

Overall (not state selected) branching ratios were measured in the SIFDT between 200 and 550 K. Just as the rate constants were relatively flat with temperature and kinetic energy, so are the branching ratios.[100,109] Charge transfer accounts for about half of the reactivity, NO^+ production for 40% and O^+ for slightly less than 10%. At total energies about 0.15 eV charge transfer becomes slightly more important (70% above 0.6 eV) at the expense of both other channels.

Formation of the $NO^+(a^3\Sigma^+)$ is 0.3 eV exothermic. This ion reacts with Ar although the ground state does not.[111] This difference allows for a determination of the branching between the two states by adding Ar upstream of the reaction inlet. Measurements by Albritton *et al.*[9] determined that less than 5% of the NO^+ was $NO^+(a^3\Sigma^+)$ at room temperature. The production of $NO^+(a^3\Sigma^+)$ was recently remeasured at AFRL to see if this channel increased at higher temperatures.[110] At both 300 and 550 K, about 0.5% of the total products or 1% of the NO^+ is in the excited state, substantially reducing the upper limit.

This appears to be a relatively simple reaction involving only 3 atoms. However, both reactants are triplets and many reaction pathways are involved. The Morokuma group has calculated the stable structures on this complicated surface and elucidated a number of important aspects of the reaction.[110] The details of the calculations are too complicated to summarize here but include the important finding that the reaction starts with an efficient early stage charge transfer to form $N(^2D) + O_2^+(X\ ^2\Pi)$ (3e). This charge transfer serves as the starting point for most of the reaction pathways

including those leading to NO^+ and O^+ products. Production of $NO^+(a\ ^3\Sigma^+)$ is found to be disfavored in accord with the experiments.

Confirmation of the $N(^2D)$ production has important implications for thermospheric chemistry. The NO concentration in that region is controlled in part by ionic processes which produce $N(^2D)$ and $N(^4S)$.[4] Most of the $N(^2D)$ produced reacts with O_2 to produce NO,

$$N(^2D) + O_2 \rightarrow NO + O. \quad (4)$$

In contrast, $N(^4S)$ leads to NO destruction because the reaction of $N(^4S)$ with O_2 is slow,

$$N(^4S) + O_2 \rightarrow NO + O. \quad (5)$$

Instead, most of the $N(^4S)$ reacts with NO,

$$N(^4S) + NO \rightarrow N_2 + O, \quad (6)$$

thereby destroying NO. Other minor processes also occur. Thus, the balance of NO in this region is strongly influenced by the ratio of $N(^4S)$ to $N(^2D)$, in part through reaction 3. Other important ionic sources of N atoms include the recombination of NO^+ and N_2^+ and the reaction of N_2^+ with O atoms.[38,41,42,112–116] With the advent of storage rings for studying dissociative recombination, product state information is now known for all of the important ionospheric reactions.

The reactions of O^+, O_2^+, N^+, N_2^+, and N_3^+ with NO have been studied to 1400 K.[117–119] During the study of the reaction of O^+ with NO in the ceramic tube, unusual kinetics was found above 1000 K, which indicated that the NO was reacting on the ceramic walls. That caused the change from a ceramic flow tube to an industrial strength quartz tube. No such problem occurred on quartz. Charge transfer is the only product in all the reactions except for the N^+ reaction where 2% O^+ and 7% N_2^+ are found in addition to the main charge transfer product.[119] The only reaction that is rapid is that of O_2^+ which occurs at half the collision rate, independent of temperature and kinetic energy within error.[7,117,120] The agreement between the dependences indicates that no type of energy influences greatly the reactivity including NO vibrations.

The charge transfer reaction of O^+ with NO is extremely slow and has been studied from 25 to 1400 K including data taken with the CRESU technique.[14,67,117,121,122] Below room temperature, the rate constant decreases with increasing temperature and by several hundred K increases substantially with temperature. The minimum rate constant is only 8×10^{-13} $cm^3\ s^{-1}$. A plot of rate constant *vs.* average translational and rotational temperature shows that temperature and kinetic energy fit on a smooth curve implying that both types of energy affect the reactivity equally. Only a small effect due to NO vibrational excitation is possible. The combined CRESU, HTFA, and drift tube data were fit to a power law plus single exponential and a power law plus double exponential. The former fits the data poorly while the latter does an exceptional job as shown in Fig. 8. Activation energies are found to be 0.25 and 2.3 eV. The low rate is attributed to poor electronic coupling; a result of the products being spin forbidden.[96] The negative temperature dependence at low temperatures

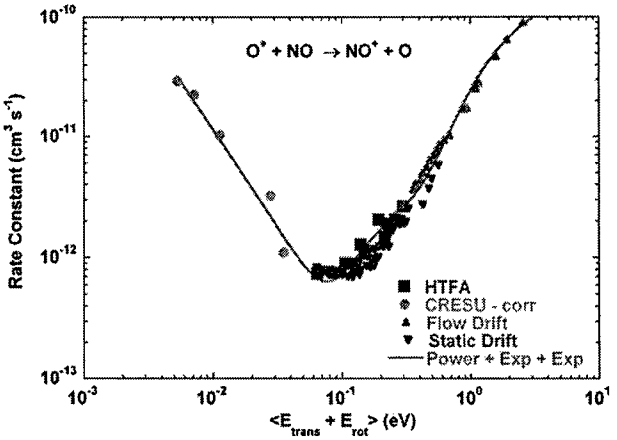

Fig. 8 Rate constants for the reaction of O^+ ions with NO as a function of average translation plus rotational energy. HTFA data are from Dotan and Viggiano[117] CRESU data are from Le Garrec *et al.*[14] flow drift tube data are from Albritton *et al.*[67] and static drift tube data are from Graham *et al.*[122] and the flowing afterglow (FA) data are from McFarland *et al.*[121] The CRESU data have been corrected for an impurity in the NO. The dashed line represents a power law fit to the CRESU data only. The solid curve represents a power law plus exponential fit to corrected CRESU plus HTFA data. Reused with permission from Itzhak Dotan, *Journal of Chemical Physics*, **110**, 4730 (1999). Copyright 1999, American Institute of Physics.

implies a mechanism involving complex formation. The lower of the two activation energies corresponds to production of the $^3A_1$ and $^3B_1$ excited states of the NO_2^+ intermediary as suggested originally by Ferguson.[123] The second activation energy corresponds to production of $NO^+(^3S)$ and $O(^3P)$ products (2.04 eV endothermic).

The reactions of N^+, N_2^+, and N_3^+ with NO have a number of similarities and have been measured from 300 to 1400 K recently.[119] All proceed exclusively by charge transfer, except the N^+ reaction which has small contributions from O^+ (1–2%) and N_2^+ (7–11%) channels. The numbers in parentheses refer to branching percentages at 300 and 500 K, respectively. All three reactions have rate constants in the 10^{-9} to 10^{-10} $cm^3\ s^{-1}$ range. Fig. 9. shows rate constants for the three reactions *vs.* total energy for both kinetic energy (9a) and pure temperature (9b).[124–127] The low energy/temperature rate constants decrease with increasing number of nitrogen atoms in the ion although the N^+ and N_2^+ rate constants are strikingly similar even though the N_2^+ reaction has competing channels and charge transfer has different energetics. The rate constants for N_3^+ are more dissimilar, although they are only a factor of 2–3 smaller than those for the smaller species.

All three reactions have negative temperature/energy dependences at low energies and a leveling or increase at higher temperatures or energies. All three reactions depend only on the total energy within our uncertainty, although it is possible that vibrational energy may hinder the reactions, *i.e.* the HTFA data are the same as or slightly smaller than those taken in the drift tube. Comparing temperature and kinetic energy dependences is more sensitive to vibrations enhancing reactivity than decreasing it, because the bulk of the reagents are still in $v = 0$. Therefore, large positive enhancements make

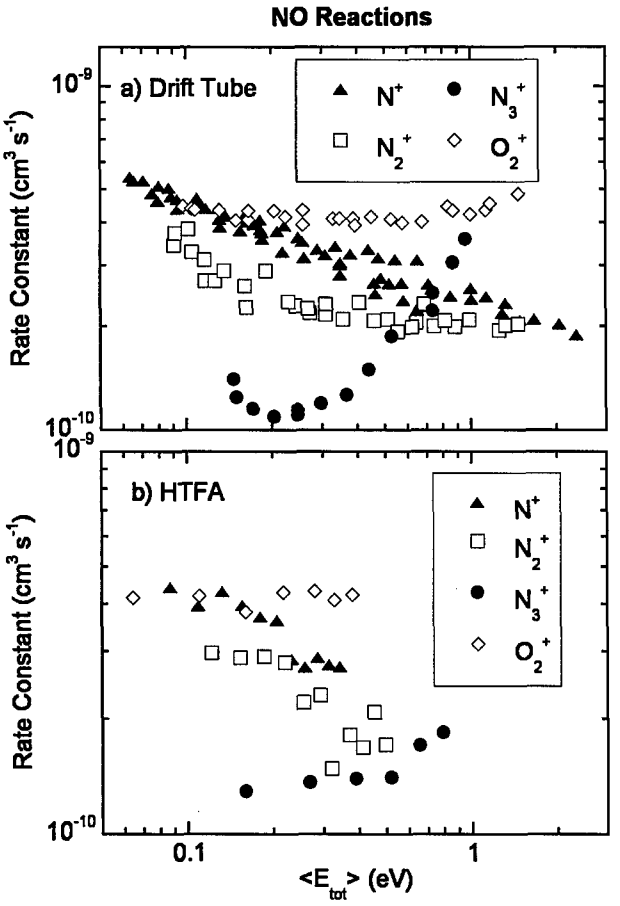

Fig. 9 Rate constants for the reactions of N_n^+ (n = 1–3) with NO as a function of average total energy. (a) Drift tube data from several sources[124,126,127,154] (b) HTFA data from Midey *et al.*[119] Reused with permission from Anthony J. Midey, *Journal of Chemical Physics*, **121**, 6822 (2004). Copyright 2004, American Institute of Physics.

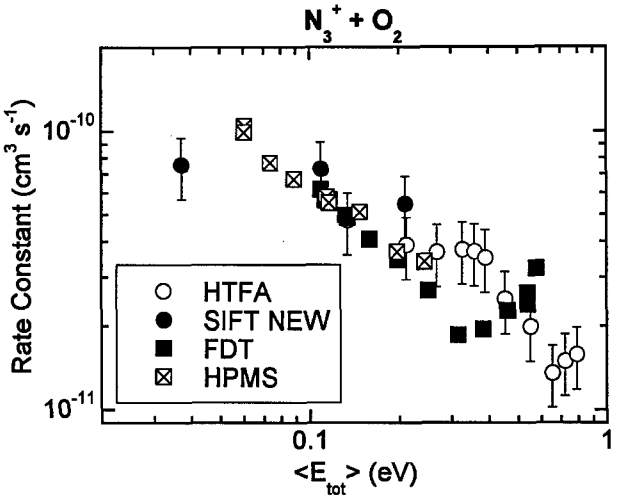

Fig. 10 Dependence of the rate constants for the reaction of N_3^+ with O_2 *vs.* average total energy. The SIFT new and HTFA data are from Popovic *et al.*,[137] the flow drift tube data (FDT) are from[127] and high pressure mass spectrometer (HPMS) data from Hiraoka.[31] Reused with permission from Svetozar Popovic, *Journal of Chemical Physics*, **121**, 9481 (2004). Copyright 2004, American Institute of Physics.

for bigger changes in the overall rate. A large negative dependence will only decrease the rate constant by the small fraction in that state.

All five reactions involving NO show similar dependences on its internal energy. By now it is clear that usually rotational and translational energy affect the reactivity similarly. For NO, it appears that v = 0 and 1 react with the same rate constants, at least to a factor of two. This is consistent with the largest Franck–Condon factors being for formation of $NO^+(X)$ in the lowest vibrational levels.[128,129] The importance of Franck–Condon factors was also apparent in the O_2 reactions discussed above in that the enhancements of the rate constants were similar for several reactions. Vibrational excitation of CO_2 decreases rate constants.[20] Two reactions involving SO_2 show somewhat different behavior.[20] Thus for the same neutral, vibrational excitation influences reactivity similarly, especially if charge transfer is involved. This is attributed mainly to Franck–Condon effects, which have been shown to be very important when the ion is state selected as shown in the work of Leone and Bierbaum, Zare, and Anderson.[72,130–136]

The final high temperature study reviewed here is that for $N_3^+ + O_2$,

$$N_3^+ + O_2 \rightarrow NO_2^+ + N_2 + 466 \text{ kJ mol}^{-1} \quad (7a)$$

$$\rightarrow NO^+ + (N_2O) + 124 \text{ kJ mol}^{-1} \quad (7b)$$

where the parentheses indicate that the neutral products are not known.[137] This reaction was studied from 120 to 1400 K and both product fractions and rate constants were studied over the whole range. In order to study the branching fractions in the HTFA, the increase in NO_2^+ was compared to the decrease in N_3^+ since other ions in the tube make NO^+ but not NO_2^+. Comparison to SIFT data at 500 K showed that this technique worked well. Extensive theoretical calculations of the mechanism were also performed and used to discuss the structure of the product in reaction (7a).

Overall rate constants for this reaction *vs.* total energy are shown in Fig. 10 including drift tube measurements.[127] In this case, total energy contains appreciable amounts of N_3^+ vibrational energy. The drift tube and HTFA results coincide indicating that all forms of energy behave similarly, probably indicative of a long lived complex controlling reactivity. The similarity in different types of energy is in an average sense. Small differences between states are hard to separate especially if some vibrations increase reactivity and others decrease it. The rate constants decrease with energy up to just under one eV and then start to increase. There appears to be a change of slope at about 0.2 eV. Other measurements are in good agreement as well.[29,31,138,139] This reaction of O_2 does not show the large enhancement observed for reactions involving charge transfer, thereby adding weight to the argument that Franck–Condon factors are very important in the rate enhancement for those reactions., *i.e.* rate enhancements are biggest if charge transfer is the dominant channel.

Before the recent measurements of reaction (7), there was contradictory information concerning the branching ratios

(NO_2^+/NO^+), with a SIFT value[139] being lower than other values.[30,139] The AFRL SIFT values showed no such disagreement indicating a problem with the previous SIFT value, where N^+ was injected into a 50% He/50% N_2 buffer to produce N_3^+. This apparently caused an artifact. The ratio of NO_2^+ to NO^+ was found to decrease exponentially from a value of 2 at 120 K to a value of 0.006 at 1400 K. There are no drift tube data to compare to but given the size of the system, total energy is expected to control the ratio. No particular importance is given to the exponential decrease at this time. The mechanism will be addressed in more detail below.

Unusual isomers

The isomer produced in reaction (7a) had been controversial.[29–31,140] Differing studies had concluded that it was either normal NO_2^+ with a central N atom or the peroxide form, NOO^+. The use of a SIFDT easily resolved this problem. The reaction was studied in the presence of Xe which was expected to have an ionization potential between the two isomers. Therefore, any NOO^+ formed would charge exchange with Xe and the ONO^+ isomer would not. This test confirmed that only NOO^+ was formed.

This result was further confirmed by detailed *ab initio* calculations of the various NO_2^+ isomers.[137] Highlights of those calculations include the finding that a linear form of NOO^+ is indeed (meta)stable, 4.51 eV about the linear ground state of ONO^+. There is a 0.89 eV barrier that prevents the isomer from dissociating into $NO^+(S^+)$ and $O(^1D)$. That channel is very slightly endothermic (0.06 eV) once NOO^+ is in its ground state. The barrier to form ONO^+ from NOO^+ is prohibitively large. The bent NOO^+ isomer is found to be a transition state. For details see Fig. 4 of ref. 137.

The calculations also looked at the stationary points on both the singlet and triplet surfaces for reaction 7. The most interesting aspects of the experimental data to reproduce are (1) the negative temperature dependence in the rate constants at low energy, (2) the shelf in the rate constants at ~0.2 to 0.5 eV, (3) the upturn in the rate constants at 0.7 eV and (4) the branching ratio. The calculations qualitatively explain all of these. Most of the reactivity is thought to occur on the singlet surface and that is shown here in Fig. 11. Negative temperature dependences are usually related to intermediates below the zero of energy that are connected to products by a barrier also below the zero of energy. INT_2 in Fig. 11 fits this profile. It is formed without barrier and connected to both the NOO^+ product through TS_2 and to the NO^+ product through TS_3. Since TS_2 is lower in energy than TS_3, the predominance of the NOO^+ product is expected. With increasing temperature/energy this predominance may be expected to diminish since both barriers are considerably below the energy of the reactants and therefore become less important as the energy is raised. An additional mechanism that may reduce the NOO^+ product occurs where there is enough energy to surmount the 0.89 eV barrier to dissociation into NO^+. The shelf at 0.2 eV is predicted by the pathway forming NOO^+ involving INT_1 and TS_1. The barrier for that pathway is 0.172 eV, remarkably similar to the threshold energy of the shelf seen in Fig. 10. The only pathway that is pertinent on the triplet surface (see Fig. 6 in the original paper[137]) is the one involving a barrier 0.58 eV above the reactants. Within the accuracy of the calculations, this is similar to the upturn at 0.7 eV. Thus, the reaction at low energy/temperature appears to proceed exclusively through INT_2 with a competition between the two sets of products. At intermediary energy the pathway involving INT_1 adds to the reactivity, and finally above 0.7 eV, the triplet pathway becomes important.

Since very little was known about the reactivity of NOO^+, the measurements were extended to 16 molecules, four of which did not react (CO_2, Kr, D_2, and N_2).[141] Of the molecules

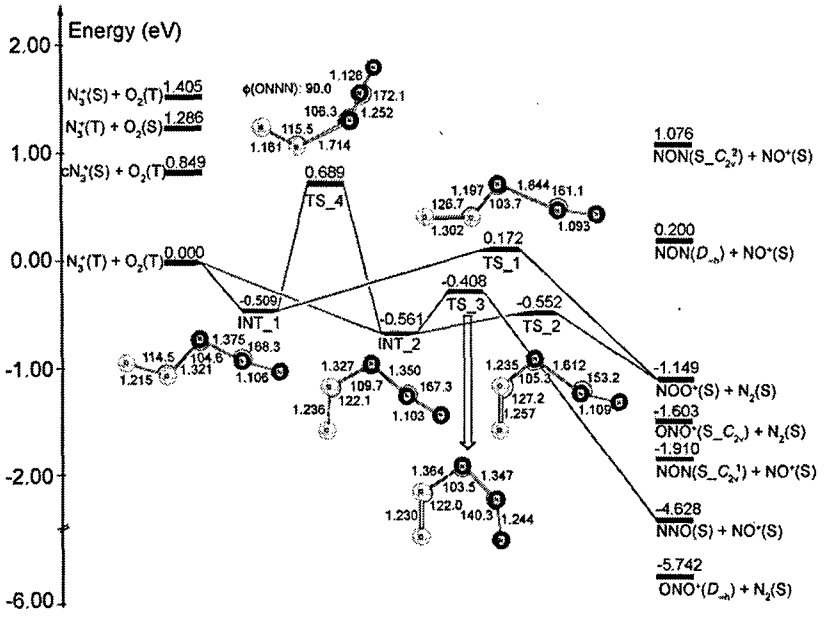

Fig. 11 Singlet potential energy surface for the reaction of N_3^+ with O_2. Reused with permission from Svetozar Popovic, *Journal of Chemical Physics*, **121**, 9481 (2004). Copyright 2004, American Institute of Physics.

that reacted (NO, C_6F_6, CS_2, CF_3I, C_3F_6, OCS, C_2H_6, Xe, SO_2, O_3, N_2O, CO) all except N_2O reacted near (>50%) the collisional limit. All measurements were performed at room temperature only. One goal of the measurements was to determine the ionization potential (IP) of NOO. Normally, that would involve change exchange experiments with both NOO^+ and NOO. However, the latter experiments are not possible. Therefore, NOO^+ was reacted with a series of simple molecules with increasing IPs and charge transfer was found for all molecules with IPs less than or equal to 11.18 eV (OCS) and was non-existent for molecules with IPs greater than 11.5 eV. This indicates that the IP of NOO is in-between these values. Calculations at the MRCISD(Q)/AVQZ level indicate that the adiabatic and vertical IPs of NOO are 10.4 and 11.7, respectively, in reasonable agreement with the measurements.[141]

Numerous other pathways were also observed. Isomerization of NOO^+ to ONO^+ is very exothermic and may have been expected to be a prominent channel. However, this was found only in the reactions with CS_2 (14%) and SO_2 (45%). The evidence for isomerization is a curved decay plot since ONO^+ does not to react with the molecules studied. The basis for the absence of isomerization may involve the excited ONO^+ dissociating into NO^+ plus two neutral products, *i.e.* ONO^+ may be formed in a very excited state and dissociate into NO^+ and O. Production of NO^+ was seen in the reaction of NO^+ (>98%), C_6F_6 (9%), CS_2 (17%), CF_3I (55%), C_3F_6 (73%), OCS (59%), Xe (97%), SO_2 (55%), O_3 (98%), N_2O, (100%), and CO (95%). The data do not address whether the O is attached to a neutral molecule.

Several of the reactions have many channels. For instance, in the reactions with OCS, C_3F_6, CF_3I, and CS_2, three, four, five and six different product ions were formed, respectively. In the Xe reaction, XeO^+ was formed—another unusual ion. The reaction with C_2H_6 proceeded by H transfer and was first observed by Matsuoka *et al.*[30] A detailed calculation of that pathway was performed but is not further discussed here.

At this stage we change focus to reactions involving negative ions, which only become important in the atmosphere at altitudes lower than approximately 100 km, *i.e.* in the mesosphere or almost equivalently D-region of the ionosphere. The early chemistry involved is generally known[1,3] but as shown below can benefit from measurements by newer techniques. Not many new studies of this chemistry have been made to date although a few examples are discussed below.

The first example of a negative ion involves another interesting peroxide isomer, $ONOO^-$. This species is formed in the reactions of CO_4^-, O_4^- and $O_2^-(H_2O)$ with NO.[27,28,142] All occur in the atmosphere. While this isomer was first identified in 1974 and is an important intermediate in the ion chemistry of the mesosphere, few reactions involving this ion had been reported. The only rate constant measured was for reaction with H,[143] although reactions with NO and CO_2 were observed.[28] It was the latter reaction that confirmed the peroxide was formed because CO_2 reacts with the product of the NO reactions and trigonal NO_3^- does not.

In order to better understand the chemistry, a study of the kinetics of 12 reactions of $ONOO^-$ was made at 200 and 300 K.[47] At 300 K, the $ONOO^-$ was made in the flow tube by injecting CO_4^- (which may be described as $O_2^-(CO_2)$) and reacting it with NO,

$$CO_4^- + NO \rightarrow ONOO^- + CO_2 \qquad (8)$$

Reaction (8) is slow; 3.6×10^{-11} cm^3 s^{-1},[27,47,144] requiring a large quantity of NO to be added to the flow tube, occasionally causing problems with product identification.

At 200 K, larger signals were obtained by injecting O_2^- into an O_2 buffer thereby forming O_4^-. At 300 K, this resulted in approximately 50% O_4^-. The reaction of $O_4^-(O_2^-O_2)$ with NO occurs near the collision value,[27]

$$O_4^- + NO \rightarrow ONOO^- + O_2. \qquad (9)$$

The larger signals and reduced quantity of NO made the measurements easier to interpret for few several systems.

No reaction was observed with NO, in contrast to the previous result. The reaction with NO_2 was found to be fast and the error in the past work therefore attributed to a small amount of NO_2 impurity in the NO. This was removed in the AFRL study by trapping the NO at low temperature. It was confirmed that $ONOO^-$ reacted with CO_2 to form CO_3^-. The rate constant is about half the collisional value at 300 K and increased to the collisional value at 200 K. Interestingly, the published heats of formation indicated this reaction was 55 kJ mol^{-1} endothermic indicating an error in at least one of the heats of formation. Since the thermochemistry of the neutrals involved is well known,[145] this meant that either the heat of formation of $ONOO^-$ [146] or CO_3^- was in error. Since the former is known only from calculations and the latter was studied extensively by laser techniques (see below), one would expect that the former was in error. However, as shown below, the problem was in the heat of formation of CO_3^-, an important intermediate in the chemistry of the lower atmosphere.

CO, H_2, CH_4, and H_2O were found not to react with $ONOO^-$. Charge transfer reactions with O_3 and NO_2 were rapid. Proton transfer from HCl was fast and from HCN was slow. The former reaction also formed O_2HCl^-, *i.e.* an NO for HCl exchange. The main product in the HCN reaction was CNO^- (74%) with a small amount of NO_2^- (12%) also produced. The reaction with SO_2 was rapid to form SO_4^- in a high energy peroxide or cluster form. The presence of the high energy isomer was determined by its reaction with NO to form SO_3^-. For the ionosphere, the important reactions are those with H, O_3, NO_2, and CO_2. Reactions involving O atoms may be important, and studies of these are planned.

Other negative ion reactions

Associative detachment reactions are important in the mesosphere since they reform electrons. A number of such reactions are important and often involve atomic neutrals like O, N or H, including those of O_2^- with O and N. These had previously been measured at NOAA using the flowing afterglow technique.[147] The rate constants were estimated to only be accurate to a factor of two.

In attempting to calibrate our system for making O and N atom measurements, the reactions of O_2^- with N and O were recently remeasured using the SIFDT technique.[148] In the

course of those measurements, two problems in the previous measurements with N atoms were found. The rate constant was found to be a factor of two smaller ones, although with the error limits the two measurements agreed. Additionally, the previous measurement indicated that only associative detachment was occurring,

$$O_2^- + N \rightarrow (NO_2) + e. \qquad (10a)$$

The new measurements found an additional channel producing O^-,

$$O_2^- + N \rightarrow O^- + NO. \qquad (10b)$$

The branching percentage for the ionic channel (10b) was found to 35%. SIFDT measurements are much easier than flowing afterglow measurements since only one ion and no source neutral is present in the flow tube. Better agreement was found for the reaction of O_2^- with O.

The final experiment to be discussed was done in collaboration with Mark Johnson's group at Yale and is the only one focusing on systems with atoms other than N or O. As mentioned above, the heat of formation of CO_3^- was in error even though the O^-–CO_2 bond strength was supposedly determined accurately through past photodissociation experiments.[149–151] However, as it turns out, those experiments were dealing with excited ions—at least in part. In the Johnson laboratory, ions are tagged with Ar molecules to ensure that they are cold.[152] This works because the Ar bond strength is weak and therefore very little internal energy leads to dissociation. Single photon action spectra ($CO_3^-(Ar) \rightarrow CO_3^- + Ar$) were performed to determine the vibrational and electronic structure. The electronic spectrum matched a previous two photon spectrum on bare CO_3^-.[150] In the two photon spectrum, all features were due to the absorption of the first photon. The agreement between the two photon spectrum and the Ar tagged spectrum indicated that (1) the Ar did not significantly disturb the CO_3^- and (2) the spectrum is "black" in the second photon. A few bands due to excited CO_3^- were identified in the spectrum of the bare CO_3^-. These could be reproduced in the Johnson laboratory.

In order to accurately determine the bond strength of O^-–CO_2, two photon experiments on both $CO_3^-(Ar)$ and $CO_3^-(Ar_2)$ were performed. The first photon was fixed at 2.067 eV and used to dissociate the Ar(s). The hot CO_3^- resulting then absorbed a variable frequency infrared photon to dissociate the CO_3^-. The signal of the resulting O^- is plotted in Fig. 12 as a function of the combined photon energy. In both systems, a sharp threshold is observed and a plateau is seen at only slightly higher photon energy. The two curves are offset by 54 meV, which is the second Ar binding energy. The shape of the curve is due to the internal energy distribution. The plateau occurs when the combined energy of the photons is large enough so that all molecules which absorb two photons dissociate into $O^- + CO_2 + Ar$ (+Ar). The threshold occurs when only the hottest molecules dissociate. The curves in the figures are Gaussian fits of the distribution and represent the data well. The bond dissociation energy for O^-–CO_2 is the plateau energy for $CO_3^-(Ar)$ minus the difference between the two curves. This compensates for the added

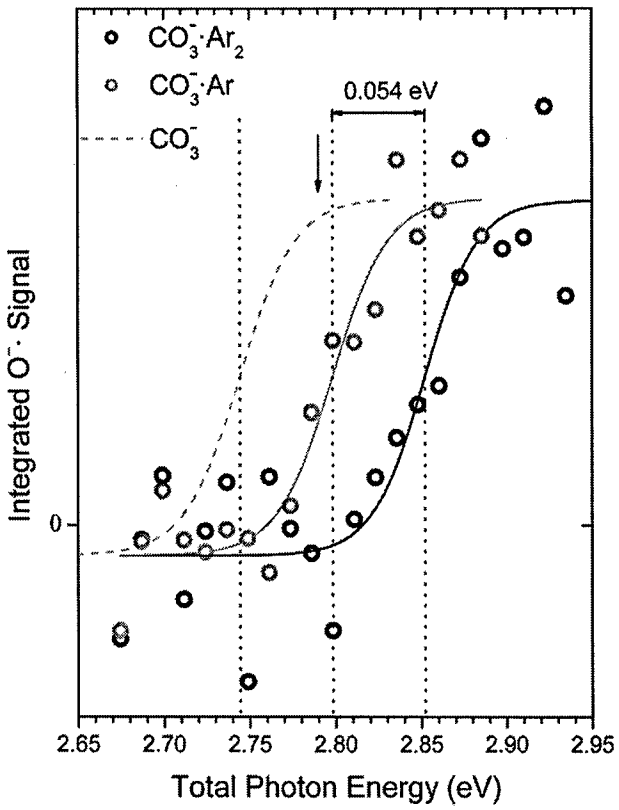

Fig. 12 O^- yield in the two photon dissociation of $CO_3^-(Ar)$ and $CO_3^-(Ar)_2$ *vs.* total photon energy. The figure is reprinted with permission from ref. 152.

Ar. The value is 2.79 ± 0.05 eV compared to the previous best value of 2.3 eV.[149] G3 calculations are in agreement with the new value of the bond strength.[47] Currently, high level calculations are being performed to determine whether the ground state of CO_3^- is C_{2v} or D_{3h}.

Conclusions

The goal of this review has been to show that while ionospheric chemistry appears to be a mature field there remains important research to be done to improve our understanding. The chemistry of atmospheric discharges starts similarly and the same studies apply. Here, a variety of improvements to previous data were presented. For a number of reactions, the range of conditions studied was increased substantially; particularly important is the temperature range which allowed internal energy dependences to be derived by comparing to drift tube data. The importance of such measurements was confirmed by modeling of ionospheric density depletions. In other instances, the chemistry had not been previously explored, *e.g.* the chemistry of the unusual isomers NOO^+ and $ONOO^-$ which are intermediates in the reaction sequence of the lower atmosphere. For other reactions, the states of the products have been measured or predicted for the first time. Particularly important are the reactions that produce N atoms including the reaction of N^+ with O_2 and dissociative recombination reactions. With detailed knowledge of ionospheric

chemistry, it can be predicted that the above studies will lead to better models of the ionosphere. More difficult to predict are the examples where errors in the chemistry exist. Two examples of such chemistry were presented; the thermodynamics of CO_3^- and the reaction of O_2^- with N atoms. These were discovered more or less serendipitously. A third example, the reaction of N^+ with O_2, was realized to be in error because of the large body of work that showed rotational and translational are equivalent in driving reactivity.

Future plans in our laboratory include studying atom reactions as a function of temperature, where little information is known. Fragmentary information exists on reactions involving $O_2(^1\Delta)$, where only two 300 K rate constants are known and the error limits are a factor of 10. Presently, it is possible to study these reactions with more accuracy and as a function of temperature. Another area worthy of new studies involves water clustering reactions. The previous studies of these important reactions were performed in flowing afterglows where the clusters were in equilibrium with each other. With the supersonic source used in our laboratory connected to the SIFDT, these can be studied more cleanly.

The study of state distributions of the products should continue in other laboratories. In addition, modern theoretical techniques are now capable of accurately calculating reaction pathways and energetics. The error in the thermodynamics of CO_3^- was discovered because the heat of formation of $ONOO^-$ was accurately calculated. Such calculations can also predict product state information when experiments do not exist. These are just a few of the potential fruitful areas for further research.

Acknowledgements

I would like to thank the many colleagues that participated in this work, both at AFRL and elsewhere. In particular I would like to thank the present AFRL team of Tom Miller, Anthony Midey, John Williamson and Paul Mundis. These collaborations made the work fun and often led to new insights. I also want to thank Eldon Ferguson and Fred Fehsenfeld for teaching me the joys of ionospheric chemistry and providing the chemical foundation to build on. I also gratefully acknowledge long term support from the AFOSR chemical dynamics program. Without that support it would not have been possible to gradually build the instrumentation needed to make these measurements.

References

1 E. E. Ferguson, F. C. Fehsenfeld and D. L. Albritton, Ion Chemistry of the Earth's Atmosphere, in *Gas Phase Ion Chemistry*, ed. M. T. Bowers, Academic, San Diego, 1979, vol 1, p. 45.
2 E. E. Ferguson, Ion-Molecule Reactions in the Atmosphere, in *Kinetics of Ion-Molecule Reactions*, ed. P. Ausloos, Plenum Publishing Corp, New York, 1979, p. 377.
3 G. C. Reid, Ion Chemistry of the D-Region, in *Advances in Atomic and Molecular Physics*, ed. D. R. Bates and B. Bederson, Academic Press, Orlando, 1976, vol 12, p. 375.
4 G. Brasseur and S. Solomon, *Aeronomy of the Middle Atmosphere*, D. Reidel, Boston, MA, 2nd edn, 1986.
5 Y. Ikezoe, S. Matsuoka, M. Takebe and A. A. Viggiano, *Gas Phase Ion-Molecule Reaction Rate Constants Through 1986*, Maruzen Company, Ltd, Tokyo, 1987.
6 V. Anicich, *An index of the literature for bimolecular gas phase cation-molecule reaction kinetics*, Jet Propulsion Laboratory, Pasadena, CA, 2003.
7 W. Lindinger, F. C. Fehsenfeld, A. L. Schmeltekopf and E. E. Ferguson, *J. Geophys. Res.*, 1974, **79**, 4753.
8 A. Chen, R. Johnsen and M. A. Biondi, *J. Chem. Phys.*, 1978, **69**, 2688.
9 D. L. Albritton, A. A. Viggiano, I. Dotan and F. C. Fehsenfeld, *J. Chem. Phys.*, 1979, **71**, 3295.
10 A. O. Langford, V. M. Bierbaum and S. R. Leone, *J. Chem. Phys.*, 1986, **84**, 2158.
11 M. A. Smith, V. M. Bierbaum and S. R. Leone, *Chem. Phys. Lett.*, 1983, **94**, 398.
12 G. Herzberg, *Molecular Spectra and Molecular Structure; I. Spectra of Diatomic Molecules*, D. Van Nostrand Co. Inc., New York, 1950.
13 *Handbook of Geophysics and the Space Environment*, ed. A. S. Jursa, National Technical Information Service, Springfield, VA, 1985.
14 J. L. Le Garrec, V. Lepage, B. R. Rowe and E. E. Ferguson, *Chem. Phys. Lett.*, 1997, **270**, 66.
15 B. R. Rowe, J. B. Marquette and C. Rebrion, *J. Chem. Soc., Faraday Trans. 2*, 1989, **85**, 1631.
16 I. W. M. Smith and B. R. Rowe, *Acc. Chem. Res.*, 2000, **33**, 261.
17 D. Gerlich, *Phys, Scripta*, 1995, **T59**, 256.
18 D. Gerlich and S. Horning, *Chem. Rev.*, 1992, **92**, 1509.
19 D. J. Levandier, Y.-H. Chiu and R. A. Dressler, *J. Chem. Phys.*, 2000, **112**, 122.
20 A. A. Viggiano and R. A. Morris, *J. Phys. Chem.*, 1996, **100**, 19227.
21 A. A. Viggiano and S. Williams, Ion-Molecule Kinetics at High Temperatures (300–1800 K): Derivation of Internal Energy Dependences, in *Advances in Gas Phase Ion Chemistry*, ed. N. G. Adams and L. M. Babcock, Academic Press, New York, 2001, vol. 4, p. 85.
22 S. Mark and D. Gerlich, *Chem. Phys.*, 1996, **209**, 235.
23 C. Nicolas, R. Torrents and D. Gerlich, *J. Chem. Phys.*, 2003, **118**, 2723.
24 D. J. Levandier, R. A. Dressler, Y. Chiu and E. Murad, *J. Chem. Phys.*, 1999, **111**, 3954.
25 H. Fu, J. Qian, R. J. Green and S. L. Anderson, *J. Chem. Phys.*, 1998, **108**, 2395.
26 S. L. Anderson, *Acc. Chem. Res.*, 1997, **30**, 28.
27 F. C. Fehsenfeld, E. E. Ferguson and D. K. Bohme, *Planet Space Sci.*, 1969, **17**, 1759.
28 F. C. Fehsenfeld and E. E. Ferguson, *J. Chem. Phys.*, 1974, **61**, 3181.
29 S. Matsuoka, H. Nakamura and T. Tamura, *J. Chem. Phys.*, 1981, **75**, 681.
30 S. Matsuoka, H. Nakamura and T. Tamura, *J. Chem. Phys.*, 1983, **79**, 825.
31 K. Hiraoka, *J. Chem. Phys.*, 1989, **91**, 6071.
32 J. R. Jasperse, *The photoelectron distribution function in the terrestrial ionosphere*, MIT Symposium on the Physics of Space Plasmas, Cambridge, MA, 1981.
33 A. A. Viggiano and F. Arnold, Ion Chemistry and Composition of the Atmosphere, in *Atmospheric Electrodynamics*, ed. H. Volland, CRC Press, Boca Raton, FL, 1995, vol. 1, p. 1.
34 A. A. Viggiano and D. E. Hunton, *J. Mass Spectrom.*, 1999, **34**, 1107.
35 E. E. Ferguson, *Radio Sci.*, 1972, **7**, 397.
36 R. S. Narcisi, A. P. Mitra, L. G. Jacchia and W. S. Newman, *Space Res.*, 1968, **8**, 360.
37 J. M. C. Plane, *Chem. Rev.*, 2003, **103**, 4963.
38 T. Mostefaoui, S. Laube, G. Gautier, C. Rebrion-Rowe, B. R. Rowe and J. B. A. Mitchell, *J. Phys. B: At. Mol. Opt. Phys.*, 1999, **32**, 5247.
39 R. Peverall, S. Rosan, J. R. Peterson, M. Larsson, A. Al-Khalili, L. Vikor, J. Semaniak, R. Bobbenkamp, A. Le Padellec, A. N. Maurellis and W. J. van der Zande, *J. Chem. Phys.*, 2001, **114**, 6679.
40 R. Peverall, S. Rosan, M. Larsson, J. R. Peterson, R. Bobbenkamp, S. L. Guberman, H. Danared, M. af Ugglas, A. Al-Khalili, A. N. Maurellis, L. Vikor and W. J. van der Zande, *Geophys. Res. Lett.*, 2000, **27**, 481.

41 J. R. Peterson, A. Le Padellec, H. Danared, G. H. Dunn, M. Larsson, R. Peverall, C. Stromholm, S. Rosan, M. af Ugglas and W. J. van der Zande, *J. Chem. Phys.*, 1998, **108**, 1978.
42 F. Hellberg, S. Rosén, R. Thomas, A. Neau, M. Larsson, A. Petrignani and W. van der Zande, *J. Chem. Phys.*, 2003, **118**, 6250.
43 A. Petrignani, P. C. Cosby, F. Hellberg, R. D. Thomas, M. Larsson and W. J. van der zande, *J. Chem. Phys.*, 2005, **122**, 014302.
44 A. A. Viggiano, S. T. Arnold and R. A. Morris, *Int. Rev. Phys. Chem.*, 1998, **17**, 147.
45 A. A. Viggiano, R. A. Morris, F. Dale, J. F. Paulson, K. Giles, D. Smith and T. Su, *J. Chem. Phys.*, 1990, **93**, 1149.
46 E. E. Ferguson, *J. Phys. Chem.*, 1986, **90**, 731.
47 A. A. Viggiano, A. J. Midey and A. Ehlerding, *Int. J. Mass Spectrom.*, 2006, in press.
48 A. A. Viggiano, R. A. Morris, J. M. Van Doren and J. F. Paulson, *J. Chem. Phys.*, 1992, **96**, 275.
49 M. Gilbert, *Combust. Flame*, 1958, **2**, 149.
50 L. A. Viehland and R. E. Robson, *Int. J. Mass Spectrom. Ion Processes*, 1989, **90**, 167.
51 D. W. Fahey, F. C. Fehsenfeld, E. E. Ferguson and L. A. Viehland, *J. Chem. Phys.*, 1981, **75**, 669.
52 R. A. Dressler, H. Meyer, A. O. Langford, V. M. Bierbaum and S. R. Leone, *J. Chem. Phys.*, 1987, **87**, 5578.
53 M. A. Duncan, V. M. Bierbaum, G. B. Ellison and S. R. Leone, *J. Chem. Phys.*, 1983, **79**, 5448.
54 E. A. Mason and E. W. McDaniel, *Transport properties of ions in gases*, John Wiley and Sons, Inc., New York, 1988.
55 A. A. Viggiano, R. A. Morris and J. F. Paulson, *J. Chem. Phys.*, 1989, **90**, 6811.
56 A. A. Viggiano, R. A. Morris and J. F. Paulson, *J. Chem. Phys.*, 1988, **89**, 4848.
57 E. E. Ferguson, F. C. Fehsenfeld and A. L. Schmeltekopf, Flowing afterglow measurements of ion-neutral reactions, in *Adv. At. Mol. Phys.*, ed. D. R. Bates, Academic, New York, 1969, vol. 5, p. 1.
58 M. McFarland, D. L. Albritton, F. C. Fehsenfeld, E. E. Ferguson and A. L. Schmeltekopf, *J. Chem. Phys.*, 1973, **59**, 6620.
59 H. W. Ellis, R. Y. Pai, E. W. McDaniel, E. A. Mason and L. A. Viehland, *At. Data Nucl. Data Tables*, 1976, **17**, 177.
60 A. A. Viggiano, R. A. Morris and E. A. Mason, *J. Chem. Phys.*, 1993, **98**, 6483.
61 A. J. Midey and A. A. Viggiano, *J. Phys. Chem. A*, 2001, **114**, 6072.
62 P. M. Hierl, J. F. Friedman, T. M. Miller, I. Dotan, M. Mendendez-Barreto, J. Seeley, J. S. Williamson, F. Dale, P. L. Mundis, R. A. Morris, J. F. Paulson and A. A. Viggiano, *Rev. Sci. Instrum.*, 1996, **67**, 2142.
63 I. Dotan and A. A. Viggiano, *J. Chem. Phys.*, 1999, **110**, 4730.
64 T. Vondrak, S. Broadly, J. M. C. Plane, B. Cosic, A. Ermoline and A. Fontijn, *J. Phys. Chem. A*, 2006, in press.
65 G. H. Wannier, *AT&T Tech. J.*, 1953, **32**, 170.
66 M. McFarland, D. L. Albritton, F. C. Fehsenfeld, E. E. Ferguson and A. L. Schmeltekopf, *J. Chem. Phys.*, 1973, **59**, 6610.
67 D. L. Albritton, I. Dotan, W. Lindinger, M. McFarland, J. Tellinghuisen and F. C. Fehsenfeld, *J. Chem. Phys.*, 1977, **66**, 410.
68 R. J. Green, J. Qian, H. T. Kim and S. L. Anderson, *J. Chem. Phys.*, 2000, **113**.
69 E. B. Anthony, W. Schade, M. J. Bastian, V. M. Bierbaum and S. R. Leone, *J. Chem. Phys.*, 1997, **106**, 5413.
70 M. Kriegel, R. Richter, W. Lindinger, L. Barbier and E. E. Ferguson, *J. Chem. Phys.*, 1988, **88**, 213.
71 J. C. Poutsma, M. A. Everest, J. E. Flad and R. N. Zare, *Appl. Phys. B: Lasers Opt.*, 2000, **71**, 623.
72 J. C. Poutsma, M. A. Everest, J. E. Flad, G. C. Jones, Jr and R. N. Zare, *Chem. Phys. Lett.*, 1999, **305**, 343.
73 M. A. Everest, J. C. Poutsma, J. E. Flad and R. N. Zare, *J. Chem. Phys.*, 1999, **111**, 2507.
74 R. J. Green, J. Xie, R. N. Zare, A. A. Viggiano and R. A. Morris, *Chem. Phys. Lett.*, 1997, **277**, 1.
75 J. Liu, B. Van Devener and S. L. Anderson, *J. Chem. Phys.*, 2003, **119**, 200.
76 J. Liu, B. Van Devener and S. L. Anderson, *J. Chem. Phys.*, 2002, **117**, 8292.
77 H.-T. Kim, J. Liu and S. L. Anderson, *J. Chem. Phys.*, 2001, **115**, 5843.
78 H.-T. Kim, R. J. Green and S. L. Anderson, *J. Chem. Phys.*, 2000, **113**, 11079.
79 J. Qian, R. J. Green and S. L. Anderson, *J. Chem. Phys.*, 1998, **108**, 7173.
80 Y.-h. Chiu, H. Fu, J.-t. Huang and S. L. Anderson, *J. Chem. Phys.*, 1996, **105**, 3089.
81 J. Qian, H. Fu and S. L. Anderson, *J. Phys. Chem. A*, 1997, **101**, 6504.
82 M. J. Frost, S. Kato, V. M. Bierbaum and S. R. Leone, *Chem. Phys.*, 1998, **231**, 145.
83 S. Kato, J. A. de Gouw, C.-D. Lin, V. M. Bierbaum and S. R. Leone, *Chem. Phys. Lett.*, 1996, **256**, 305.
84 J. A. d. Gouw, L. N. Ding, M. J. Frost, S. Kato, V. M. Bierbaum and S. R. Leone, *Chem. Phys. Lett.*, 1995, **240**, 362.
85 S. Kato, M. J. Frost, V. M. Bierbaum and S. R. Leone, *Rev. Sci. Instrum.*, 1993, **64**, 2808.
86 A. A. Viggiano and R. A. Morris, *J. Chem. Phys.*, 1993, **99**, 3526.
87 A. L. Schmeltekopf, E. E. Ferguson and F. C. Fehsenfeld, *J. Chem. Phys.*, 1968, **48**, 2966.
88 A. A. Viggiano, J. M. Van Doren, R. A. Morris, J. S. Williamson, P. L. Mundis, J. F. Paulson and C. E. Dateo, *J. Chem. Phys.*, 1991, **95**, 8120.
89 I. Dotan, A. A. Viggiano and R. A. Morris, *J. Chem. Phys.*, 1992, **96**, 7445.
90 A. A. Viggiano, R. A. Morris, J. S. Paschkewitz and J. F. Paulson, *J. Am. Chem. Soc.*, 1992, **114**, 10477.
91 R. A. Morris and A. A. Viggiano, *J. Phys. Chem.*, 1994, **98**, 3740.
92 A. A. Viggiano, R. A. Morris, T. Su, B. D. Wladkowski, S. L. Craig, M. Zhong and J. I. Brauman, *J. Am. Chem. Soc.*, 1994, **116**, 2213.
93 P. M. Hierl, I. Dotan, J. V. Seeley, J. M. Van Doren, R. A. Morris and A. A. Viggiano, *J. Chem. Phys.*, 1997, **106**, 3540.
94 A. A. Viggiano, J. M. Van Doren, R. A. Morris, J. S. Williamson, P. L. Mundis and J. F. Paulson, *J. Chem. Phys.*, 1991, **95**, 8120.
95 R. A. Dressler and A. A. Viggiano, Charge Transfer-Fundamentals, in *Encyclopedia of Mass Spectrometry - Organic Ions*, ed. M. L. Gross, R. Caprioli and N. Nibbering, Elsevier, Amsterdam, 2005, vol. 4.
96 R. A. Dressler, D. J. Levandier, S. Williams and E. Murad, *Comments At. Mol. Phys.*, 1998, **34**, 43.
97 R. Johnsen and M. A. Biondi, *J. Chem. Phys.*, 1973, **59**, 3504.
98 E. V. Mishin, W.J. Burke and A. A. Viggiano, *J. Geophys. Res.*, 2004, **109**, A10301.
99 I. Dotan, P. M. Hierl, R. A. Morris and A. A. Viggiano, *Int. J. Mass Spectrom. Ion Phys.*, 1997, **167/168**, 223.
100 F. Howorka, I. Dotan, F. C. Fehsenfeld and D. L. Albritton, *J. Chem. Phys.*, 1980, **73**, 758.
101 A. O. Langford, V. M. Bierbaum and S. R. Leone, *Space Sci.*, 1985, **33**, 1225.
102 R. Johnsen, H. L. Brown and M. A. Biondi, *J. Chem. Phys.*, 1970, **52**, 5080.
103 D. Smith, N. G. Adams and T. M. Miller, *J. Chem. Phys.*, 1978, **69**, 308.
104 A. L. Farragher, *Trans. Faraday Soc.*, 1970, **66**, 1411.
105 J. W. Dreyer and D. Perner, *Chem. Phys. Lett.*, 1971, **12**, 299.
106 R. A. Guettler, G. C. Jones, L. A. Posey, N. J. Kirchner, B. A. Keller and R. N. Zare, *J. Chem. Phys.*, 1994, **101**, 3763.
107 A. O'Keefe, G. Mauclaire, D. Parent and M. T. Bowers, *J. Chem. Phys.*, 1986, **84**, 215.
108 J. C. Tully, Z. Herman and R. Wolfgang, *J. Chem. Phys.*, 1971, **54**, 1730.
109 A. A. Viggiano, W. B. Knighton, S. Williams, S. T. Arnold, A. J. Midey and I. Dotan, *Int. J. Mass Spectrom.*, 2003, **223–224**, 397.
110 A. J. Midey, A. A. Viggiano, P. Zhang, S. Irle and K. Morokuma, *J. Phys. Chem. A*, 2006, **110**, 3080.
111 I. Dotan, F. C. Fehsenfeld and D. L. Albritton, *J. Chem. Phys.*, 1979, **71**, 3289.
112 M. McFarland, D. L. Albritton, F. C. Fehsenfeld, E. E. Ferguson and A. L. Schmeltekopf, *J. Geophys. Res.*, 1974, **79**, 2925.
113 D. G. Torr, N. Orsini, M. R. Torr, W. B. Hanson, J. H. Hoffman and J. C. G. Walker, *J. Geophys. Res.*, 1977, **82**, 1631.
114 E. E. Ferguson, F. C. Fehsenfeld, P. D. Goldan, A. L. Schmeltekopf and H. I. Schiff, *Planet. Space Sci.*, 1965, **13**, 823.

115 S. L. Guberman, The Dissociative Recombination of N_2^+. In *Dissociative Recombination of Molecular Ions with Electrons*, ed. S. L. Guberman, Kluwer/Plenum Academic Press, New York, 2003, p. 187.
116 A. Le Padellec, N. Djuric, A. Al-Khalili, H. Danared, A. M. Derkatch, A. Neau, D. B. Popovic, S. Rosén, J. Semaniak, R. Thomas, M. af Ugglas and M. Larsson, *Phys. Rev. A*, 2001, **64**, 012702.
117 I. Dotan and A. A. Viggiano, *J. Chem. Phys.*, 1999, **110**, 4730.
118 A. J. Midey and A. A. Viggiano, *J. Chem. Phys.*, 1999, **110**, 10746.
119 A. J. Midey, T. M. Miller and A. A. Viggiano, *J. Chem. Phys.*, 2004, **121**, 6822.
120 W. Lindinger, D. L. Albritton, F. C. Fehsenfeld and E. E. Ferguson, *J. Geophys. Res.*, 1975, **80**, 3725.
121 M. McFarland, D. L. Albritton, F. C. Fehsenfeld, A. L. Schmeltekopf and E. E. Ferguson, *J. Geophys. Res.*, 1974, **79**, 2005.
122 E. Graham, R. Johnsen and M. A. Biondi, *J. Geophys. Res.*, 1975, **80**, 2338.
123 E. E. Ferguson, Review. In *Interactions between Ions and Molecules*, ed. P. Ausloos, Plenum, New York, 1974, p. 320.
124 D. W. Fahey, I. Dotan, F. C. Fehsenfeld, D. L. Albritton and L. A. Viehland, *J. Chem. Phys.*, 1981, **74**, 3320.
125 W. Dobler, H. Ramler, H. Villinger, F. Howorka and W. Lindinger, *Chem. Phys. Lett.*, 1983, **97**, 553.
126 F. Howorka, D. L. Albritton and F. C. Fehsenfeld, N_2 + NO k *vs.* KE, , in *Proceedings of the Symposium on Atomic and Surface Physics, Salzburg, Austria, February 2–10, 1980*, ed. W. Lindinger, F. Howorka and F. Egger, STUDIA, A-6020, Innsbruck, 1980, p. 249.
127 W. Lindinger, *J. Chem. Phys.*, 1976, **64**, 3720.
128 R. W. Field, *J. Mol. Spec.*, 1973, **47**, 194.
129 D. L. Albritton, A. L. Schmeltekopf and R. N. Zare, *J. Chem. Phys.*, 1979, **71**, 3271.
130 R. N. Zare, *Science*, 1998, **279**, 1875.
131 J. C. Poutsma, M. A. Everest, J. E. Flad and R. N. Zare, *Appl. Phys. B*, 2000, **71**, 623.
132 M. A. Everest, J. C. Poutsma and R. N. Zare, *J. Phys. Chem.*, 1998, **102**, 9593.
133 M. A. Everest, J. C. Poutsma, J. E. Flad and R. N. Zare, *J. Chem. Phys.*, 1999, **111**, 2507.
134 H. Fu, J. Qian, R. J. Green and S. L. Anderson, *J. Chem. Phys.*, 1998, **108**, 2395.
135 S. Kato, J. A. d. Gouw, C.-D. Lin, V. M. Bierbaum and S. R. Leone, *Chem. Phys. Lett.*, 1996, **256**, 305.
136 S. Kato, J. A. d. G.-D. Lin, V. M. Bierbaum and S. R. Leone, *J. Chem. Phys.*, 1996, **105**, 5455.
137 S. Popovic, A. J. Midey, S. Williams, A. Fernandez, A. A. Viggiano, P. Zhang and K. Morokuma, *J. Chem. Phys.*, 2004, **121**, 9481.
138 D. B. Dunkin, F. C. Fehsenfeld, A. L. Schmeltekopf and E. E. Ferguson, *J. Chem. Phys.*, 1971, **54**, 3817.
139 D. Smith, N. G. Adams and T. M. Miller, *J. Chem. Phys.*, 1978, **69**, 308.
140 S. Matsuoka, H. Nakamura and T. Tamura, *J. Chem. Phys.*, 1981, **75**, 681.
141 A. J. Midey, A. I. Fernandez, A. A. Viggiano, P. Zhang and K. Morokuma, *J. Chem. Phys.*, 2006, in press.
142 D. W. Fahey, H. Bohringer, F. C. Fehsenfeld and E. E. Ferguson, *J. Chem. Phys.*, 1982, **76**, 1799.
143 F. C. Fehsenfeld, *J. Chem. Phys.*, 1975, **63**, 1686.
144 A. A. Viggiano, R. A. Morris and J. F. Paulson, *J. Chem. Phys.*, 1989, **91**, 5855.
145 *NIST Chemistry WebBook, NIST Standard Reference Database No. 69*, ed. P. J. Linstrom and W. G. Mallard, National Institute of Standards and Technology, Gaithersburg, MD, 2003, vol. (http://webbook.nist.gov).
146 A. M. Mak and M. W. Wong, *Chem. Phys. Lett.*, 2005, **403**, 192.
147 F. C. Fehsenfeld, A. L. Schmeltekopf, H.I. Schiff and E. E. Ferguson, *Planet. Space Sci.*, 1967, **15**, 373.
148 J. C. Poutsma, A. J. Midey and A. A. Viggiano, *J. Chem. Phys.*, 2006, **124**, 074301.
149 J. T. Snodgrass, C. M. Roehl, A. M. van Koppen, W. E. Palke and M. T. Bowers, *J. Chem. Phys.*, 1990, **92**, 5935.
150 J. T. Moseley, P. C. Cosby and J. R. Peterson, *J. Chem. Phys.*, 1976, **65**, 2512.
151 D. E. Hunton, M. Hofmann, T. G. Lindeman and A. W. Castleman, Jr, *J. Chem. Phys.*, 1985, **82**, 134.
152 J. C. Bopp, J. M. Headrick, J. R. Roscioli, M. A. Johnson, A. J. Midey and A. A. Viggiano, *J. Chem. Phys.*, 2006, in press.
153 P. M. Hierl, I. Dotan, J. V. Seeley, J. M. Van Doren, R. A. Morris and A. A. Viggiano, *J. Chem. Phys.*, 1997, **106**, 3540.
154 W. Dobler, H. Ramler, H. Villinger, F. Howorka and W. Lindinger, *Chem. Phys. Lett.*, 1983, **97**, 553.